Optics Communications 452 (2019) 233–237

Contents lists available at ScienceDirect

Optics Communications

journal homepage: www.elsevier.com/locate/optcom

Fiber laser based on a fiber Bragg grating and its application in high-temperature sensing

Fengqin Huang [a], Tao Chen [a,b,*], Jinhai Si [a], Xuantung Pham [a,c], Xun Hou [a]

[a] Key Laboratory for Physical Electronics and Devices of the Ministry of Education & Shaanxi Key Lab of Information Photonic Technique, School of Electronics & Information Engineering, Xi'an Jiaotong University, No.28, Xianning West Road, Xi'an, 710049, China
[b] Xi'an Jiaotong University Suzhou Academy, Suzhou, 215125, China
[c] Le Quy Don Technical University, Hanoi, 122314, Viet Nam

ARTICLE INFO

Keywords:
Optical fiber lasers
Fiber Bragg gratings
High temperature sensors

ABSTRACT

We demonstrated a linear-cavity fiber laser using a fiber Bragg grating (FBG) fabricated by femtosecond laser and a Sagnac loop as cavity mirrors. The temperature sensing response of the fiber laser was characterized by placing the FBG in a high-temperature environment. The stability of the fiber laser at high temperature was improved after the FBG was annealed at 1100 °C. The fiber laser can work stably as a temperature sensor at 1000 °C and its temperature sensing sensitivity is approximately 15.9 pm/°C from 300 °C to 1000 °C.

1. Introduction

Temperature sensors have widely applications in industrial fields. The most popular temperature sensors are electrical sensors including thermoelectric thermometer, electrical resistance thermometer, and so on. Optical sensors are getting more attention due to their advantage of immunity to electromagnetic interference. Fiber Bragg grating (FBG) sensors as one of optical sensors have particular merits of multiplexing capabilities, the ability of quasi-distributed sensing and resistance to corrosion. FBG can be used to realize sensing by measuring its reflection or transmission spectra directly. The other method is to measure the wavelength of the fiber laser based on FBG. Compared with the former, the latter has additional advantages, such as narrow linewidth, which enhances the resolution for wavelength shift, and high signal-to-noise ratio benefiting for precise measurements [1–3]. Fiber lasers based on FBGs have been widely used as hydrophones [4], temperature sensors [5] etc.

In many fields such as petrochemicals, high-temperature creep and aerospace, high temperature sensing are greatly needed. Owing to that the traditional FBGs will be erased at above 400 °C, FBG sensors and FBG-based fiber laser sensors are not suitable for high-temperature sensing. The traditional FBGs are usually fabricated by long-pulse UV lasers and result from color center formations. These types of FBGs referred to as type I gratings.

Many methods have been proposed to increase the temperature resistance of FBGs fabricated by long-pulse UV lasers. One method is to form type IIa FBGs, which are induced by introducing negative refractive index modulation into the fiber core via successive exposure to type I gratings. This type of grating can work at 700 °C [6]. A distributed Bragg reflector (DBR) fiber laser with a cavity length of 13 mm based on a Type IIa Bragg grating was reported and shown to operate stably at 600 °C [7]. Another method is to induce regenerated gratings which are obtained by thermally annealing type I gratings. The regenerated gratings have a higher sustainable temperature of up to 1000 °C [8,9]. DBR fiber lasers composed by thermally regenerated fiber gratings can withstand temperatures up to 750 °C [10].

In recent years, femtosecond lasers have been effectively used as light sources in processing FBGs [11–14]. A high reflective FBG could be inscribed by femtosecond laser within less than 60 s using the method of direct point-by-point [15]. It costs less than 1 min even few seconds to make a saturated FBG using the method of phase mask [14,16,17] depending on the fabrication conditions. FBGs fabricated using femtosecond lasers have many unique advantages compared to those fabricated by conventional UV lasers, including no photosensitivity requirement for the fiber and wonderful thermal stability [18,19]. FBGs induced by high-intensity ultrafast IR laser can work at temperatures in excess of 1000 °C [18]. FBGs fabricated by femtosecond laser have also been used to construct fiber lasers. An Erbium fiber laser based on intracore femtosecond-written FBG has been demonstrated [20]. A distributed Bragg reflector fiber laser fabricated by femtosecond laser inscription realized single-mode, single-polarization operation at temperatures in excess of 600 °C [21]. Although regenerated FBGs and FBGs made by femtosecond lasers can work at 1000 °C, to the best of our knowledge, no one has reported FBG-based fiber lasers that can operate at 1000 °C.

* Corresponding author at: Key Laboratory for Physical Electronics and Devices of the Ministry of Education & Shaanxi Key Lab of Information Photonic Technique, School of Electronics & Information Engineering, Xi'an Jiaotong University, No.28, Xianning West Road, Xi'an, 710049, China.
E-mail address: tchen@mail.xjtu.edu.cn (T. Chen).

https://doi.org/10.1016/j.optcom.2019.05.046
Received 8 January 2019; Received in revised form 15 May 2019; Accepted 21 May 2019
Available online 23 May 2019

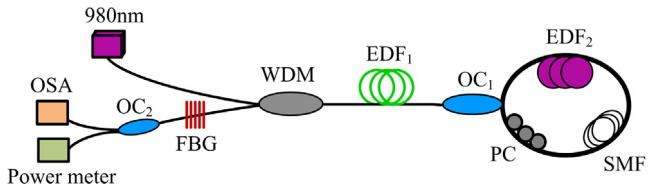

Fig. 1. (Color on line) Schematic diagram of the fiber laser. WDM: wavelength division multiplexer; OC: optical coupler; EDF_1: erbium-doped fiber (gain); EDF_2: unpumped erbium-doped fiber; SMF: single mode fiber; PC: polarization controller; OSA: optical spectrum analyzer.

In this paper, we demonstrate a fiber laser based on an FBG fabricated by femtosecond laser and a Sagnac loop. The temperature sensing response of the fiber laser is characterized. The results show that annealing the FBG at 1100 °C improved the stability of the fiber laser at high temperatures, and the fiber laser can work stably as a temperature sensor at 1000 °C. The center wavelength of the fiber laser increases with the temperature increasing and has a quadratic dependence on temperature from room temperature to 1000 °C. The dependence of the center wavelength of fiber laser on the temperature is nearly linear over 300 °C to 1000 °C range and the temperature sensing sensitivity in this temperature range is approximately 15.9 pm/°C according to the linear fitting.

2. Experimental setup

The schematic diagram of the fiber laser is shown in Fig. 1. The fiber laser consists of a 980-nm pump laser diode, a wavelength division multiplexer (WDM) and a length of Er-doped fiber (1.6 m, ESF-7/125, Nufern) as the gain of the fiber laser. The cavity of the fiber laser is formed by an FBG and a Sagnac loop. The Sagnac loop is comprised of a polarization controller (PC), a single-mode fiber (2 m, SMF-28, Corning), a 2-m length of unpumped Er-doped fiber (EDF) (EDFC-980-HP, Nufern), and an optical coupler of 50/50. The output laser is split into two beams by a 10/90 optical coupler. Ten percent of the fiber laser output is sent to an optical spectrum analyzer (OSA; Yokogawa, AQ6370D; spectral resolution 20 pm) to measure the output spectra, and the remaining power is transmitted to a power meter to measure the output power. The unpumped Er-doped fiber is used as a saturable absorber to improve the stability of the fiber laser [22,23]. The Sagnac loop incorporated with the unpumped EDF can be regarded as a passive self-tracking narrow multiband optical filter [22,24] and be able to stabilize the output of the fiber laser when two counter-propagate waves formed a standing wave in it. Because the longitudinal mode interval of the fiber laser was 17.2-MHz and the full-width-at-half maximum bandwidth of the induced filter was 14.8-MHz, the fiber laser satisfied the mode-selection condition.

The FBG was induced by 50-fs laser pulses generated by an amplified Ti: sapphire laser (Libra-USP-HE, Coherent, USA) at a center wavelength of 800 nm and 1-kHz repetition rate with a Gaussian spatial profile. The maximal single-pulse energy is about 3.5 mJ. The Gaussian beam is focused by a cylindrical lens with a focal length of 25 mm and then passed through a zero-order nulled phase mask with period $\Lambda_m = 2.142$ μm into the standard telecom fiber core. Femtosecond laser can induce Type I and Type II grating structures in fibers depending on the laser intensity of femtosecond laser, and only Type II grating structures can withstand the high temperature up to 1000 °C [18]. The threshold light intensity for forming Type II FBG is higher than that for forming Type I FBG. In order to fabricate Type II FBG, the distance between the fiber and phase mask was set to less than 1 mm to produce a multiple beam interference-field pattern with a higher intensity than that generated by two-beam interference [25]. The femtosecond laser was set at a power of 750 mW. FBGs were fabricated by the interval exposure of femtosecond laser, which can suppress the thermal effects and increase the reflectivity and formation efficiency of FBGs [26]. The exposure times are controlled by a mechanical beam shutter with the minimum open time of less than 20 ms and timing accuracy of 1 ms, the exposure time and interval time were set to 0.1 s and 5 s, respectively. The reflectivity of the FBG as a function of exposure time in interval exposure mode has been shown in Fig. 2(a). The reflectivity of the FBG firstly increases with the increase of exposure time and then reached saturation at an exposure time of about 0.8 s. The saturated reflectivity is about 83.0%.

In our demonstrated fiber laser, only a low-reflective FBG was needed and used as the fiber laser output mirror. The low reflective FBG was obtained by cutting a saturated Type II FBG rather than decreasing the exposure time or power of the femtosecond pulse laser. This ensured the low reflective FBG contain Type II structures as many as possible. The exposure time of the saturated Type II FBG was 0.9 s. The lengths of the saturated FBG and after it was being cut off a portion were 3.3 mm and 1.4 mm, respectively. The spectra of the saturated FBG before and after cutting are shown in Fig. 2(b). The 3 dB bandwidth and reflectivity of the two FBG are 1.060 nm, 83.3% and 1.032 nm, 55.9%, respectively. The transmission spectra of the FBG before and after cutting are shown in the set of Fig. 2(b). The blue shift of FBG reflection spectra after cutting was observed. This may because the saturated FBG fabricated by femtosecond laser was apodized due to the Gaussian beam profile of femtosecond laser, and the center and peripheral portion of the FBG own different effective refractive indexes thereby different Bragg wavelengths [18]. The central portion structures of the FBG may arise from laser-induced damage at high laser intensity, for example micro voids, i.e. Type II grating structures, which result in a decrease of refractive index [18,27]. The peripheral portion structures of the FBG may arise from color center, i.e. Type I structures, which results in an increase of refractive index [18].

Fig. 2(c) shows the output spectrum of the fiber laser at room temperature at a pump power of 600 mW. The 3 dB bandwidth is 0.032 nm, which is much narrower than that of the FBG. The output signal-to-noise ratio is more than 60 dB. The output power of the fiber laser was 29 mW. We verified that when no unpumped EDF was present in the Sagnac loop, the wavelength of the fiber laser output became unstable.

3. Results and discussion

The performance of the FBG-based fiber laser was tested at different temperatures with a pump power of 600 mW. The FBG was placed in a tube furnace that can be operated from room temperature to 1200 °C. During the heating process, the temperature was increased at intervals of 100 °C and kept 60 min at each temperature to observe the stability of the fiber laser output after the temperature had stabilized. Fig. 3(a) shows the variation in wavelength at different temperatures. At temperatures from room temperature to 800 °C, the fiber laser wavelength quickly reached a stable value when the temperature of the furnace reached the set temperature. In contrast, the wavelength of the fiber laser was red-shifted at 900 °C and 1000 °C, even when the temperature was kept constant for 100 min. Next, we increased the temperature of the tube furnace to 1100 °C and annealed the FBG for 10 min. After annealing, the wavelength of fiber laser remained stable at 1000 °C after keeping the temperature constant for 40 min. Fig. 3(b) and (c) show the wavelength and intensity of the fiber laser before and after annealing at 900 °C and 1000 °C, respectively. At both 900 °C and 1000 °C, the intensity of the fiber laser was similar before and after annealing, while obvious differences in wavelength were observed. More specifically, at both 900 °C and 1000 °C, the wavelength was clearly red-shifted before annealing and became more stable after annealing.

Next, we increased the temperature directly to 1000 °C from room temperature and tested the long-term thermal stability of the fiber laser while it operated for 300 min at 1000 °C. The variation in the

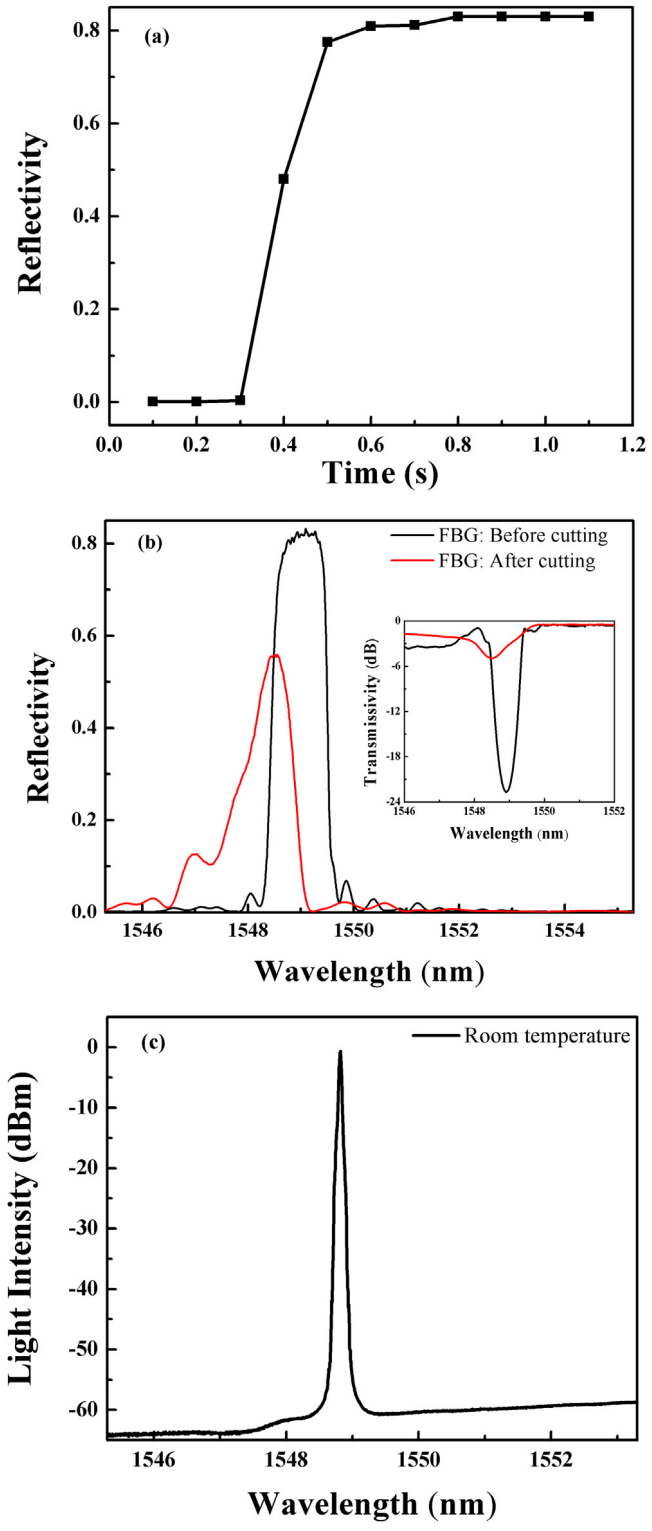

Fig. 2. (Color on line) (a) Reflectivity of the FBG as a function of exposure time in interval exposure mode. (b) Reflection spectra of the FBG before and after cutting. Inset: The transmission spectra of the FBG before and after cutting. (c) The output spectrum of the fiber laser at a pump power of 600 mW.

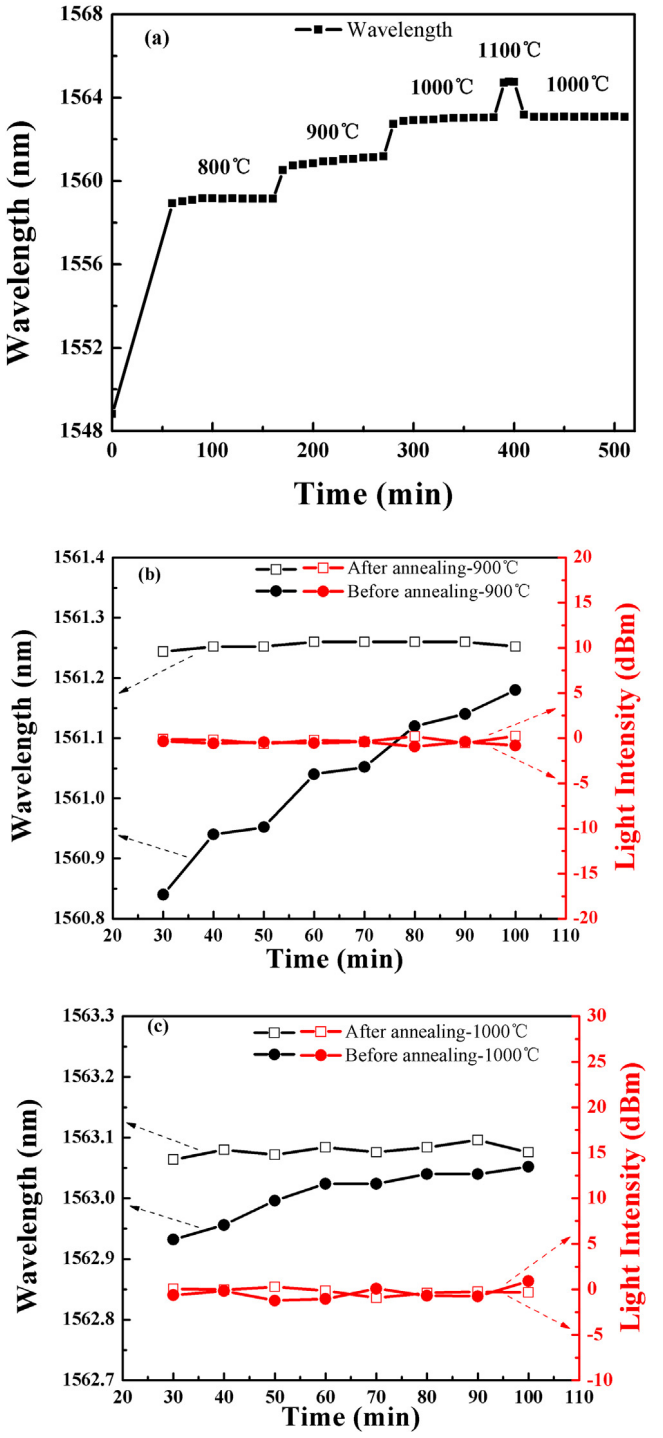

Fig. 3. (a) Variation in wavelength at different temperatures before and after annealing at 1100 °C. (b) Details of the wavelength and intensity of the fiber laser at 900 °C before and after annealing. (c) Details of the wavelength and intensity of the fiber laser at 1000 °C before and after annealing. The squares and circles represent the recorded data. (For interpretation of the references to color in this figure legend, the reader is referred to the web version of this article.)

wavelength and intensity of the fiber laser with time are shown in Fig. 4. The wavelength and intensity became stable after 30 min. The wavelength showed a small fluctuation of less than 0.05 nm. The above results imply that the fiber laser achieved stable output at high temperatures up to 1000 °C after the FBG was annealed at 1100 °C.

The temperature sensing characteristics of the FBG-based linear-cavity fiber laser were tested. The temperature of the tube furnace was increased from 100 °C to 1000 °C in intervals of 100 °C in the heating process. Each temperature was maintained for 60 min to obtain spectra. The temperature was then decreased from 1000 °C to 100 °C in intervals of 100 °C to characterize the behavior of the fiber laser output

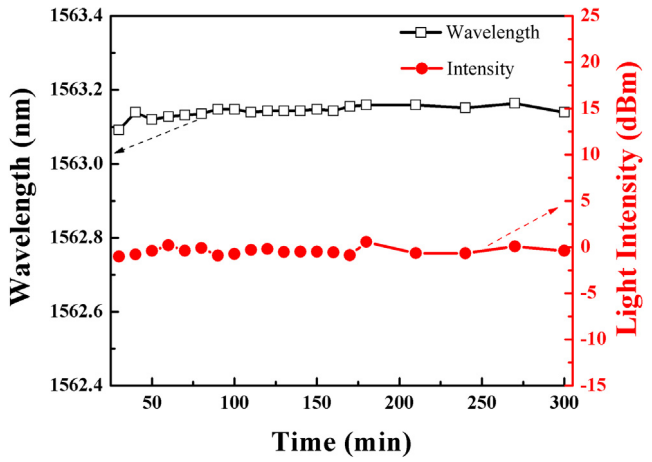

Fig. 4. (Color on line) Variation in fiber laser wavelength and intensity as the laser worked at 1000 °C for 300 min. The squares and circles represent the recorded data.

during the cooling process. Again, each temperature was maintained for 60 min to obtain spectra.

Fig. 5(a) shows the laser spectra at different temperatures during the heating process. The variation in laser intensity with temperature during the heating and cooling processes is shown in the inset of Fig. 5(a). During the heating and cooling processes, the fiber laser intensity showed only small fluctuations of less than 1.1 dB. Fig. 5(b) shows the center wavelength of the linear-cavity fiber laser as a function of temperature from room temperature to 1000 °C. The black triangles and red inverted triangles represent the recorded data during heating and cooling processes, respectively, and the solid curves represent their quadratic fits. The curves for cooling and heating almost completely overlap. The center wavelength of the linear-cavity fiber laser increases with the temperature increasing and has a quadratic dependence on temperature. The quadratic behavior of the FBG-based fiber laser output from room temperature to 1000 °C may be due to the quadratic behavior of FBG temperature coefficients [28,29]. The inset of Fig. 5(b) shows the linear fitting results of the temperature–wavelength curves from 300 °C to 1000 °C. The solid curves represent their linear fits (R^2 = 99.9%). The good linear relationship of fiber laser wavelengths and temperatures makes the temperature sensor demodulation easier from 300 °C to 1000 °C. The temperature sensitivity of the fiber laser wavelength is about 15.9 pm/°C for both heating and cooling processes from 300 °C to 1000 °C. Consequently, we achieved a fiber laser with good temperature sensing ability at 1000 °C.

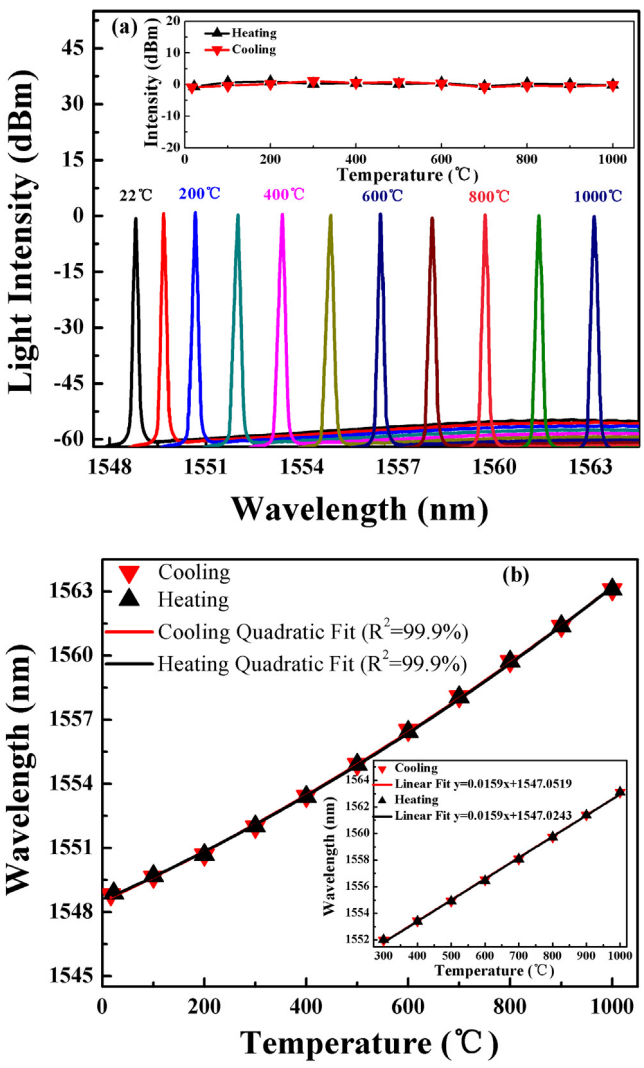

Fig. 5. (a). Spectra at different temperatures during the heating process. Inset: Variation in laser intensity with temperature during the heating and cooling processes. (b). Center wavelength of the linear-cavity fiber laser as a function of temperature from room temperature to 1000 °C. The solid curves represent the quadratic fit. Inset: center wavelength of the laser as a function of temperature from 300 °C to 1000 °C. The solid curves represent the linear fit. The black triangles and red inverted triangles represent the recorded data. (For interpretation of the references to color in this figure legend, the reader is referred to the web version of this article.)

4. Conclusion

We developed a linear-cavity fiber laser based on an FBG fabricated by femtosecond laser, and tested its temperature sensing characteristics. The fiber laser worked stably at 1000 °C after annealing at 1100 °C and its wavelength had a quadratic dependence on temperature from room temperature to 1000 °C. The temperature–wavelength had a good linear relationship from 300 °C to 1000 °C. According to the linear fitting, the average sensing sensitivity was estimated to be about 15.9 pm/°C from 300 °C to 1000 °C. The temperature–wavelength curves showed good repeatability between the heating and cooling processes. Thus the linear-cavity fiber laser has good sensing repeatability. The results of this work imply that the fiber laser can be applied at high temperatures up to 1000 °C.

Acknowledgments

The authors acknowledge the National Key Research and Development Program of China (Grant No. 2017YFB1104600); Suzhou Science and Technology Planning Project, China (Grant No. SYG201622); Key Research and Development Program of Shaanxi province, China (Grant No. 2017ZDXM-GY-120); Fundamental Research Funds for the Central Universities (Grant No. XJJ2016016).

References

[1] Z. Yin, L. Gao, S. Lin, L. Zhang, F. Wu, L. Chen, X. Chen, Fiber ring laser sensor for temperature measurement, J. Lightwave Technol. 28 (23) (2010) 3403–3408.

[2] A.D. Kerseey, M.A. Davis, H.J. Patrick, M.L. Blanc, K.P. Koo, C.G. Askins, M.A. Putnam, E.J. Friebele, Fiber grating senors, J. Lightwave Technol. 15 (8) (1997) 1442–1463.

[3] Y. Yu, L. Lui, H. Tam, W. Chung, Fiber-laser-based wavelength-division multiplexed fiber bragg grating sensor system, IEEE Photonics Technol. Lett. 13 (7) (2001) 702–704.

[4] D.J. Hill, P.J. Nash, D.A. Jackson, D.J. Webb, S.F. OŃeill, I. Bennion, L. Zhang, Fiber laser hydrophone arry, in: Proceedings of SPIE, 1999.

[5] Jaehoon Jung, Hui Nam, Byoungho Lee, Jae Oh Byun, Nam Seong Kim, Fiber bragg grating temperature sensor with controllable sensitivity, Appl. Opt. 38 (13) (1999) 2752–2754.

[6] N. Groothoff, J. Canning, Enhanced type IIA gratings for high-temperature opration, Opt. Lett. 29 (20) (2004) 2360–2362.
[7] Y. Ran, F.R. Feng, Y.Z. Liang, L. Jin, B.O. Guan, Type IIa bragg grating based ultra-short DBR fiber laser with high temperature resistance, Opt. Lett. 40 (24) (2015) 5706–5709.
[8] S. Bandyopadhyay, J. Canning, M. Stevenson, K. Cook, Ultrahigh-temperature regenerated gratings in boron-codoped germanosilicate optical fiber using 193 nm, Opt. Lett. 33 (16) (2008) 1917–1919.
[9] K. Cook, C. Smelser, J. Canning, G. le Garff, M. Lancry, S. Mihailov, Regenerated femtosecond fiber bragg gratings, Proc. Spie. 8351 (2012) 8351111–1–835111–6.
[10] R. Chen, A. Yan, M. Li, T. Chen, Q. Wang, J. Canning, K. Cook, K.P. Chen, Regenerated distributed bragg reflector fiber lasers for high-temperature operation, Opt. Lett. 38 (14) (2013) 2490–2492.
[11] J. Thomas, E. Wikszak, T. Clausnitzer, U. Fuchs, U. Zeitner, S. Nolte, A. Tünnermann, Inscription of fiber bragg gratings with femtosecond pulses using a phase mask scanning technique, Appl. Phys. A 86 (2007) 153–157.
[12] S.J. Mihailov, C.W. Smelser, D. Grobnic, R.B. Walker, P. Lu, H. Ding, J. Unruh, Bragg gratings written in All-SiO_2 and ge-doped core fibers with 800-nm femtosecond radiation and a phase mask, J. Lightwave Technol. 22 (1) (2004) 94–100.
[13] Y. Du, T. Chen, Y. Zhang, R. Wang, H. Cao, K. Li, Fabrication of phase-shifted fiber bragg grating by femtosecond laser shield method, IEEE Photonics Technol. Lett. 29 (24) (2017) 2143–2146.
[14] W. Cui, T. Chen, J. Si, F. Chen, X. Hou, Femtosecond laser processing of fiber bragg gratings with photo-induced gradient-index assisted focusing, J. Micromech. Mingcroe 24 (2014) 075015(5pp).
[15] A. Martinez, M. Dubov, I. Khrushchev, I. Bennion, Direct writing of fiber bragg gratings by femtosecond laser, Electron. Lett. 40 (19) (2004) 1170–1172.
[16] Stephen J. Mihailov, Christopher W. Smelser, Ping Lu, Robert B. Walker, Dan Grobnic, Huimin Ding, George Henderson, Fiber bragg gratings made with a phase mask and 800-nm femtosecond radiation, Opt. Lett. 28 (12) (2003) 995–997.
[17] Rui Yang, Yong-Sen Yu, Chao Chen, Qi-Dai Chen, Hong-Bo Sun, Rapid fabrication of microhole array structured optical fibers, Opt. Lett. 36 (19) (2011) 3879–3881.
[18] C.W. Smelser, S.J. Mihailov, D. Grobnic, Formation of type i-IR and type II-ir gratings with an ultrafast IR laser and a phase mask, Opt. Express 13 (14) (2005) 5377–5386.
[19] C. Liao, Y. Li, D.N. Wang, T. Sun, K.T. V.Grattan, Morphology and thermal stability of fiber bragg gratings for sensor applications written in H_2-free and H_2-loaded fibers by femtosecond laser, IEEE Sens. J. 10 (11) (2010) 1675–1681.
[20] E. Wikszak, J. Thomas, J. Burghoff, B. Ortac, J. Limpert, S. Nolte, Erbium fiber laser based on intracore femtosecond-written fiber bragg grating, Opt. Lett. 31 (16) (2006) 2390–2392.
[21] Y. Lai, A. Martinez, I. Khrushchev, I. Bennion, Distributed bragg reflector fiber laser fabricated by femtosecond laser inscription, Opt. Lett. 31 (11) (2006) 1672–1674.
[22] J. Liu, J. Yao, J. Yao, T.H. Yeap, Single-longitudinal-mode multiwavelength fiber ring laser, IEEE Photonics Technol. Lett. 16 (4) (2004) 1020–1022.
[23] Y. Cheng, J.T. Kringlebotn, W.H. Loh, R.I. Laming, D.N. Payne, Stable single-frequency traveling-wave fiber loop laser with integral saturable-absorber-based tracking narrow-band filter, Opt. Lett. 20 (8) (1995) 875–877.
[24] K. Zhang, J.U. Kang, C-band wavelength-swept single-longitudinal-mode erbium-doped fiber ring laser, Opt. Express 16 (18) (2008) 14173–14179.
[25] S.J. Mihailov, C.W. Smelser, D. Grobnic, R.B. Walker, Ping Lu, Huimin Ding, James Unruh, Bragg gratings written in All-SiO_2 and ge-doped core fibers with 800-nm femtosecond radiation and a phase mask, J. Lightwave Technol. 22 (1) (2004) 95–100.
[26] Cui Wei, Si Jin-hai, Chen Tao, Yan Fei, Chen Feng, Hou Xun, Suppression of the thermal effects in the femtosecond laser processing of fiber bragg gratings, Chin. Phys. Lett. 30 (10) (2013) 104207.
[27] Saulius Juodkazis, Hiroaki Misawa, Tomohiro Hashimoto, Eugene G. Gamaly, Barry Luther-Davies, Laser-induced microexposion confined in a bulk of silica: Formation of nanovoids, Applied Physics Letters. 88 (20) (2006) 201909.
[28] C. Liao, D. Wang, Y. Li, T. Sun, K.T.V. Grattan, Temporal thermal response of type II-IR fiber Bragg gratings, Appl. Opt. 48 (16) (2009) 3001–3007.
[29] G.M.H. Flockhart, R.R.J. Maier, J.S. Barton, W.N. MacPherson, J.D.C. Jones, K.E. Chisholm, L. Zhang, L. Bennion, L. Read, P.D. Foote, Quadratic behavior of fiber bragg grating temperature coefficients, Appl. Opt. 43 (13) (2004) 2744–2751.